Simulation-based optimization of PCM melting temperature to improve the energy performance in buildings

Mohammad Saffari[1], Alvaro de Gracia[2], Cèsar Fernández[3], Luisa F. Cabeza[1*]

[1]*GREA Innovació concurrent, INSPIRES Research Centre, University of Lleida, Pere de Cabrera s/n, 25001, Lleida, Spain.*

[2]*Departament d'Enginyeria Mecànica, Universitat Rovira i Virgili, Av. Països Catalans 26, 43007, Tarragona, Spain.*

[3]*Departament d'Informàtica i Enginyeria Industrial, INSPIRES Research Centre, Universitat de Lleida, Lleida, Spain.*

[*]*Corresponding author: lcabeza@diei.udl.cat*

Abstract

Globally, a considerable amount of energy is consumed by the building sector. The building envelope can highly influence the energy consumption in buildings. In this regard, innovative technologies such as thermal energy storage (TES) can help to boost the energy efficiency and to reduce the CO_2 emissions in this sector. The use of phase change materials (PCM), due to its high heat capacity, has been the centre of attention of many researchers. A considerable number of papers have been published on the application of PCM as passive system in building envelopes. Researches have shown that choosing the PCM melting temperature in different climate conditions is a key factor to improve the energy performance in buildings. In the present paper, a simulation-based optimization methodology will be presented by coupling EnergyPlus and GenOpt with an innovative enthalpy-temperature (h-T) function to define the optimum PCM peak melting temperature to enhance the cooling, heating, and the annual total heating and cooling energy performance of a residential building in various climate conditions based on Köppen-Geiger classification. Results show that in a cooling dominant climate the best PCM melting temperature to reduce the annual energy consumption is close to the maximum of 26ºC (melting range of 24ºC-28ºC), whereas in heating dominant climates PCM with lower melting temperature of 20ºC (melting range of 18ºC-22ºC) yields higher annual energy benefits. Moreover, it was found that the proper selection of PCM melting temperature in each climate zone can lead to notable energy savings for cooling energy consumption, heating energy consumption, and total annual energy consumption.

Keywords: Passive cooling; GenOpt; building energy simulation; PCM optimum melting.

1. Introduction

The building envelope has a crucial impact on the energy conservation [1]. Globally, space heating and cooling account for over one-third of all energy consumed in buildings, increasing to as much as 50% in cold climate region [2]. Further on, a boom in the cooling energy demand is expected as a result of growing urbanization and wealth [3] which may lead to urban heat island (UHI) effects [4] and, on the other hand, the global warming due to climate change and its corresponding side effects such as extreme heatwave periods [5] are great influencing factors of this rapid temperature rise.

This goal could be approached by taking advantage of innovative technologies such as thermal energy storage (TES) [6]. The application of TES yields better system performance and reliability, better energy efficiency, economic benefits, thermal comfort for occupants, and less CO_2 emissions [7]. TES systems are classified into three categories: thermochemical, sensible, and latent heat storage.

Thermochemical storage relies on thermochemical materials (TCM) undergoing either a physical reversible process involving two substances or reversible chemical reactions. In comparison to sensible and PCM, TCM has higher energy densities and lower volume of the storage material which results in more compact design. However, further research is required to apply this technology in buildings. Solé et al. [8] discussed the potential of TCM for building applications.

By the way, sensible heat is the simplest way of storing thermal energy by applying a temperature gradient to a solid or liquid media to store or release heat. Water has been used as the most common material for sensible heat storage. Additionally, for building applications other materials such as concrete, brick, and natural stones have been extensively used in building construction worldwide. However, for sensible heat storage in buildings massive materials are required which could be a drawback [9].

By the advent of technology and material design, today, latent heat storage is a popular means for passive design of buildings [10]. Latent heat storage depends on the material phase change enthalpy to accumulate heat within a small temperature range, providing greater energy density than that obtainable with sensible heat storage over the same temperature gradient. However, in some materials volumetric expansions may happen during the melting process [11]. Materials with a solid-liquid phase change, which are appropriate for heat or cold storage in building envelopes, are generally referred to as phase change material (PCM) [12]. The PCM technology due to its exclusive assets for thermal regulation of buildings has been the centre of attention of many researchers [13,14]. An important feature that differentiates the PCM from other typical thermal mass materials with sensible heat is the capability of storing high amounts of heat in small temperature range due to its high heat capacity. However, appropriate material selection is of a high importance to properly apply it into buildings. PCMs are classified into two main categories: organic and inorganic. Examples of the organic PCMs are paraffin, fatty acids and the polyethylene glycol. Advantages of organic PCMs are: negligible or non subcooling, chemical and thermal stability, and non-corrosiveness, and their disadvantages are: low phase change enthalpy, low thermal conductivity, and flammability. Examples of inorganic PCMs are salt hydrates [15] that have greater change enthalpy, however, they have some drawbacks such as: subcooling, corrosion, phase separation, phase segregation, and lack of thermal stability [12,16]. So that, according to all properties mentioned above, material selection should be based on the application requirements. For further information about the available PCMs for building applications one can refer to researches carried out by Cabeza et al. [17] and Barreneche et al. [18].

PCM can be incorporated into building construction materials by direct incorporation, immersion, shape-stabilized PCM, form-stable composite PCM and encapsulation which are categorized into macroencapsulation and microencapsulation [19,20]. Macroencapsulation means inclusion of PCM in a macroscopic containment (usually larger than 1 cm in diameter) such as tubes, pouches, spheres, panels or other containers. In microencapsulation, solid or liquid particles of 1 μm-1000 μm are encapsulated in a thin, high molecular weight polymeric film. Then, the enclosed particles can be incorporated in any matrix that is adaptable with the encapsulating film and adoptable with both PCM and the matrix [12,17,19].

In most applications, PCMs are microencapsulated [17] to avoid the movement of liquid phase PCM and on the other hand to avoid its contact with the surrounding and not to adversely affect e.g. the construction material. The main advantages of microencapsulation of PCM are improvement of heat transfer to the surrounding due to large surface to volume ratio of the capsules and the enhancement of cycling stability since phase separation is limited to microscopic distances. Further on, the leakage and evaporation problems are solved in this method and the loss of PCM under construction work e.g. cutting the wallboard or screwing is negligible. In addition, they could be integrated into other materials to form composite materials [12].

PCMs can be incorporated into building construction materials in various ways to provide passive cooling benefits such as gypsum plasterboard with microencapsulated paraffin [21] which is a unique solution to enhance thermal capacity of lightweight buildings, plaster with microencapsulated paraffin [22] that could be applied on the surface of the walls, concrete with microencapsulated paraffin [23], shape-stabilized paraffin panels [24], PCM bricks [25] and wood with PCM [26]. Additionally, PCMs have vast applications for building components such as slabs [27], floors [28], blinds and windows [29,30].

In buildings the TES could be applied either as a passive [10] or as an active system [31]. Both of these approaches could be appropriate and their implementation depends on some factors such as product availability, cost, climatic conditions, and energy prices [32]. However, high levels of energy efficiency in building envelope elements could be attained by passive design approach as an integrated design by taking advantage of sun as a clean and renewable source of energy. In winter, PCM can be melted during the sunny hours and store the solar energy, and late on the stored heat could be released through its solidification process. Hence, PCM melting temperature should be low enough to be melted during winter sunny hours. On the other hand, in summer, PCM through its melting process prevents cooling peak load to the indoor environment. PCM is solidified during night time and hence charged for the following day. In this case, solidification temperature of PCM has to be high enough so the PCM can be charged by free cooling at night.

The application of passive PCM systems to improve the heating and cooling energy performance in buildings has been growing rapidly over the last two decades [33]. The passive PCM technology can be applied in different parts of a building as an integrated passive design. Baetens et al. [34] reviewed some possible applications of PCM technology integrated into buildings materials such as wallboards, concrete, and thermal insulation. However, using PCM-enhanced building envelopes for passive cooling has been popular among researchers [35,36].

As an example, an experimental and numerical study was carried out by Jamil et al. [37] to investigate the potential of PCM in decreasing the zone air temperature and enhancing occupant thermal comfort in a naturally ventilated house located in Melbourne, Australia. In their experimental study, PCM with melting temperature of 25ºC (melting range of 23ºC-27ºC) was installed between ceiling insulation and plasterboard of a bedroom. Their results showed 34% reduction of thermal discomfort hours in the room with PCM inclusion. Afterwards, they performed numerical simulation to analyse the impact of occupants behaviour on the effectiveness of PCM technology. It was found that, if occupants appropriately open the windows at night time to let cool air in and during day maintain the internal doors closed, the thermal discomfort could be reduced by 52%.

The principal functionality of the PCM technology is to reduce the HVAC demand in mechanically ventilated buildings, or to moderate the indoor air temperature providing higher air quality for occupants by enhancing the thermal mass of the envelope [38]. The thermal behaviour of buildings is associated with complex physical phenomena and their performance is highly corresponded to the indoor and outdoor boundary conditions, especially, when the PCM is integrated into the building envelopes. For this reason, building simulation tools are invaluable and necessary to analyse and evaluate the energy performance and comfort conditions, specifically in buildings with renewable and innovative integrated passive technology. Moreover, it should be highlighted that today, the simulation technology has turned to be a strategic tool for policymaking [39,40] since it can help to promote a more sustainable and secure built environment with the capability of simulating a wider range of parameters in the scale of a city [41,42], for instance.

Researches have shown that selecting the PCM melting temperature in different climate conditions is a determining factor to improve the energy performance and/or thermal comfort in naturally [43] and mechanically [44] ventilated buildings. For instance, Ascione et al. [43] investigated the cooling energy performance of buildings with PCM-enhanced envelopes in some European regions (mainly warm temperature climates). Various melting temperatures of PCM (26ºC to 29ºC) were considered and eventually the highest cooling energy savings (2.5% to 7.2%) and comfort were obtained when the PCM melting at 29°C was incorporated into the walls. Along the same lines, Lei et al. [44] performed a parametric study to reduce the cooling needs in buildings located in tropical regions by means of PCM. Simulation results were shown that the application of PCM melting at 28ºC can reduce the annual heat gains by 21% to 32%, and it was highlighted that the selection of proper PCM melting point regulates the energy savings. With the same objectives, Alam el al. [45] carried out parametric analysis to find out the impacts of the PCM technology on the cooling and heating energy performance of buildings under Australian weather conditions. Buildings enhanced with PCM with six different peak melting temperatures (20ºC-25ºC) were simulated under different weather conditions and it was shown that the energy savings are highly influenced by the PCM melting point and the climatic region. As an example, for the heating season in Adelaide (June to Aug), PCM with 20ºC melting point yielded higher energy savings whereas for the cooling season (Dec to Feb) this temperature raised to 25ºC. Furthermore, they stated that the effectiveness of PCM is strongly dependent on local weather.

Further on, Saffari et al. [46] found that the PCM melting at 27ºC could save the cooling energy by 43%-66% in a building prototype with residential HVAC schedule, nevertheless, for the heating period PCM with lower melting point (23ºC) appeared to be more effective.

It can be seen from the existing literature that several attempts have been made to analyze the benefits of passive PCM system to improve the thermal comfort and energy performance of buildings in different countries. Most studies in this field have used parametric method to investigate the influence of different PCM melting temperatures on the summer cooling energy performance and/or winter heating energy performance.

In such parametric methods, some independent variables are fixed and only one variable changes to optimize the cost function. Even though, parametric studies could be useful for early stage design decisions of buildings; nevertheless, it may lead to partial energy improvement due to non-linear interactions of input variables on simulated results and it could be very time-consuming and computationally expensive [47]. Currently, in available literature, little discussion has been made on the energy optimization of PCM-enhanced passive buildings addressing the appropriate melting temperature of PCM taking into account various climate conditions. As an example, using multi-dimensional optimization, Soares et al. [48] investigated the annual and monthly heating and cooling performance of building prototypes located in warm temperate climates. They found that 10%-62% savings in energy consumption can be achieved utilizing PCM passive technology, with higher benefits in the Mediterranean climates and lower benefits in cold and humid regions.

The utilization of building optimization for real-world design challenges is in its early stage of development [47], however, in recent years, there has been a substantial growth towards the use of optimization techniques for sustainable building design [49]. This could be because of, on one hand, the advancement of computational power, and, on the other hand, industry is realizing the strong potential of optimization methods, as stated by Evins [50]. Single-objective and multi-objective optimization studies are gaining interest and they have been increasingly used for building design applications to optimize for example the energy performance in buildings, among which the building envelope optimization has been prominent [51,52].

In the present paper, a single-objective optimization method coupled with an innovative PCM enthalpy-temperature (h-T) function will be presented to find out the optimum PCM melting temperature according to the outdoor boundary conditions. Additionally, it is intended to show that the use of PCM passive system in the building envelopes with optimized peak melting temperature in each climate zone can yield energy savings while still ensuring indoor thermal comfort, in both heating dominant and cooling dominant climates.

2. Methodology

2.1. Overview

The simulation-based optimizations were carried out using EnergyPlus whole-building energy simulation coupled with a generic optimization program (GenOpt). Computations were performed on a cluster with 32x6core Intel(R) Xeon(R) processors at 2.00GHz with 48 Gigabyte memory running EnergyPlus 8.4.0 under CentOS release 6.3 - 2.6.32 x86_64 GNU/Linux. In Section 2.2, the reference building prototype is described. The PCM characterization and the innovative h-T function are explained in Section 2.2.1. In Section 2.2.2 the HVAC system and schedule are explained. In Sections 2.3 and 2.4 the simulation and optimization tools features and methodologies are described, and eventually in Section 2.5 the climate zone classifications are explained. Figure 1 shows an overall scheme of the whole methodology.

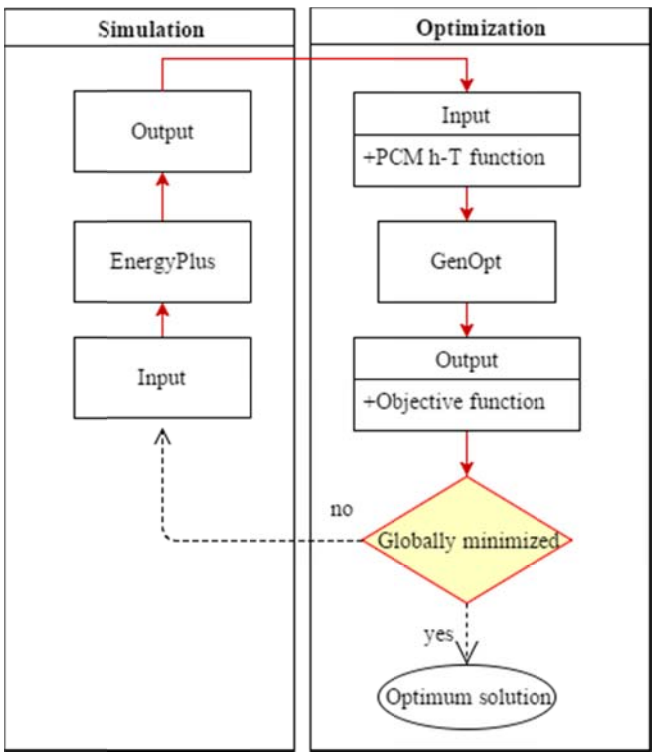

Figure 1. Methodology workflow.

2.2. Reference building

A suitable building model had to be selected to carry out the simulation in different weather conditions. On this basis, a multi-family residential apartment was selected from ASHRAE Standard 90.1- 2013 prototype building models and slightly modified [53]. The ASHRAE

Standard 90.1 prototype building models were developed by Pacific Northwest National Laboratory in support of the U.S. Department of Energy (DOE) Building Energy Codes Program. These building prototypes are simulated in different climate zones and maybe mapped to other climate locations for international use [54]. The mid-rise apartment building is a 3100 m^2 four-story building (Figure 2).

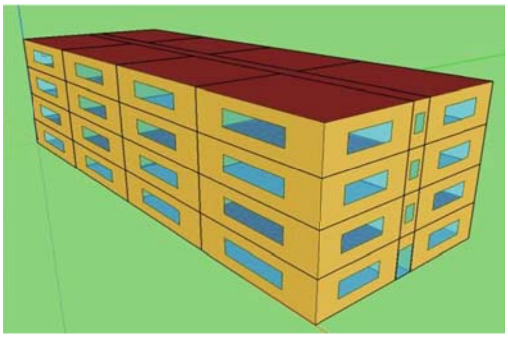

Figure 2.Reference building (mid-rise apartment).

Each floor has four conditioned residential units and a corridor, however, the first floor has an office zone which has a different occupancy period and fraction and period. The building has a rectangular shape (46.32 m × 16.91 m), with aspect ratio of 2.74, window-to-wall ratio of 20%, and floor-to-ceiling height of 3 m. Insulation entirely applied above roof deck and exterior walls are steel-framed. To integrate the PCM into the building, the building envelope is slightly modified and PCM gypsum boards were installed on the inner surface of the exterior walls and roof. Tables 1 and 2, show external vertical walls and roof construction properties with inclusion of PCM. Further information regarding the baseline building simulated in EnergyPlus, including building envelope components, building internal loads and infiltration could be found in references [54] and [55].

Table 1. Exterior walls construction.

Material	d [m]	λ [W/m·K]	ρ [kg/m^3]	C_p [J/kg·K]	R [W/m^2·K]
Stucco	0.0254	0.72	1856	840	-
Gypsum board	0.0159	0.16	800	1090	-
Insulation	-	-	-	-	1.036
PCM	0.0125	0.20	800	1200	-
Gypsum board	0.0159	0.16	800	1090	-

Table 2. Roof construction.

Material	d [m]	λ [W/m·K]	ρ [kg/m^3]	C_p [J/kg·K]	R [W/m^2·K]
Built-up roofing	0.0095	0.16	1120	1460	-
Insulation	-	-	-	-	4.318
PCM	0.0125	0.20	800	1200	-
Metal surface	0.0008	45.28	7824	500	-

2.2.1. PCM characterization

Commercially available plasterboard, suitable for drywall construction applications with about 30 wt. % of microencapsulated paraffinic PCM was selected. The latent heat capacity of 12-mm-thick of such product is around 90 Wh/m^2 which is available in two different melting points: 23 ºC and 26 ºC [56]. In order to simulate the PCM impact on the building energy consumption, the h-T curve of the selected PCM has to be introduced to EnergyPlus. Accordingly, the enthalpy method was used based on an equation which was proposed by Feustel (see Eq.1) [57,58] to construct the h-T curve of the PCM, introducing physical properties of Knauf® smartboard (Table 3).

$$h(T) = c_{p,const}T + \frac{h_2 - h_1}{2} \times \left\{ 1 + \tanh\left[\frac{2\beta}{\tau}(T - T_m) \right] \right\} \quad \text{(Eq. 1)}$$

where C_p is specific heat [kJ/kg·K], T is temperature [$^{\circ}$C], h is specific enthalpy [kJ/kg], Β is inclination [--], τ is width of the melting zone [K], and T_m is melting temperature [ºC].

Table 3. Physical properties of the Knauf smartboard® containing PCM [56].

Physical property	Value
Specific heat	1.2 kJ/kg·K
Thermal conductivity at 20 ºC	0.20 W/m·K
Thermal conductivity at 35 ºC	0.19 W/m·K
Shift range of the PCM	23 ºC or 26 ºC
Enthalpy of fusion of the PCM	110 J/g
Latent heat capacity ΔH	330 kJ/m^2

To study a wide range of PCM melting temperature, hypothetical PCM peak melting temperatures were considered from 20 ºC to 26 ºC with reference temperature at -20 ºC and melting range of 4 ºC. In addition, the PCM enthalpy was considered constant and density change due to phase change was negligible. In current literature, for optimizing the PCM melting temperature, different PCM h-T curves are created and introduced to the simulation software each time when a new temperature is analysed. In the present paper, a new methodology is presented to iteratively select PCM h-T curve which reduces the time-consuming process of h-T curve introduction to EnergyPlus at the beginning of each simulation with different PCM peak melting points, hence, simulation and optimization are continued until the optimum h-T curve is found (Figure 3). This process increases the simulation and optimization speed and also enhances the precision of finding the optimum PCM melting temperature.

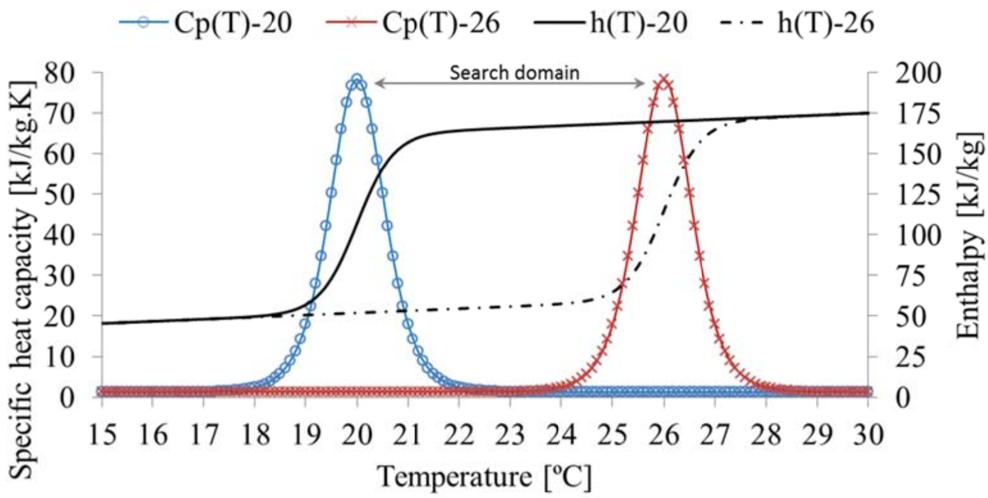

Figure 3. The iterative PCM melting temperature selection scheme.

To implement this method, the h-T values were written in the form of a series of continuous functions and were implemented into the pre-processing stage of the optimization (Eq. 2). A continuous function is referred to a function for which sufficiently small changes in the independent variables result in arbitrarily small changes in the objective function.

$$T \triangleq \left\{ T_{opt} \in \mathbf{R}^n \middle| T_{\min}{}^{i} \leq T_{opt}{}^{i} \leq T_{\max}{}^{i}, i \in \{1,\ldots,n\} \right\}, \qquad \text{(Eq. 2)}$$

where $20 \leq T_{\min} < T_{\max} \leq 26$, and $T_{opt} = T_{ref} \pm \mathbf{R}$

where T is a set of optimum PCM peak melting temperatures (T_{opt}), T_{min} and T_{max} are the minimum and maximum allowed temperatures for the PCM peak melting point.

2.2.2 HVAC system

A packaged terminal heat pump (PTHP) with constant volume fan control, direction expansion (DX) cooling coil and electric heat pump according to baseline building HVAC system types recommendations of ANSI/ASHRAE/IES Standard 90.1-2013 [59] was selected. HVAC system schedules were matched to the occupancy schedules, and to control the indoor air quality, for all zones, a dual set point thermostat with dead-band operative temperature control was selected according to the recommended indoor temperatures for energy calculations of BS EN 15251 [60]. The thermostat control was set to 20 ºC for heating and 26 ºC for cooling, as recommended for residential buildings and living spaces. Furthermore, relative humidity ratios for dehumidification and humidification were considered to be 60% and 25%, respectively, within the recommended design criteria of BS EN 15251 [60] for the humidity in occupied spaces.

2.3. Energy simulation

A set of numerical simulations were performed using EnergyPlus v8.4 [61]. This whole-building energy simulation software is a powerful building energy simulation program for modelling the energy performance in buildings. EnergyPlus takes advantage of both BLAST and DOE-2 programs. It owns many featured characteristics such as heat balance load calculations, integrated loads, system and plant calculations in same time step, user-configurable HVAC system description, simple input and output data formats to facilitate the virtualization of the results [62], simulation of PCM and materials with variable thermal conductivity [63]. Additionally, new modules and/or control strategies could be developed and integrate into the program as subroutines [64]. Also, there are plenty of options for outside and inside surface convection algorithms, advanced infiltration, ventilation, room air and multi-zone airflow calculations, environmental emissions and developed economic evaluation including energy costs, and life cycle costs [65]. Further on, several advanced human thermal comfort algorithms are included in the software to model the indoor air quality and thermal comfort of occupants [65]. To simulate PCM in EnergyPlus, a conduction finite difference (CondFD) solution algorithm must be used. This algorithm discretizes the building envelope into various nodes which could be introduced optionally depending on the required accuracy, and numerically solves the heat transfer equations by use of a finite difference method (FDM) which could be selected between Crank-Nicholson or fully implicit [66–68]. To include the specific heat change due to phase change process, the CondFD method is coupled with an enthalpy-temperature function, which reads the user inputs of enthalpies at different temperatures [69]. Since an iterative implicit scheme is used for CondFD, the node enthalpies get renewed at each iteration, and then they are used to make a variable Cp.

A validated building energy simulation is essential to properly analyse the heat transfer and thermal comfort in simulated buildings. In this regard, EnergyPlus PCM algorithms were verified and validated against analytical verification (Stefan Problem), comparative testing (against Heating 7.3) and empirical validation (DuPont Hotbox) by Tabares-Velasco et al.

[70,71]. According to their findings, some cautions should be taken into account when simulating PCM such as: (1) short time steps equal or less than 3 minutes should be used; (2) PCM with strong hysteresis could not be accurately simulated; and (3) if accurate hourly analysis is needed, smaller node space (equal to 1/3 of the default value) should be used [70]. Moreover, in many studies, simulation results obtained by PCM model of EnergyPlus were validated against experimental data. For example, some authors [45,72] validated the EnergyPlus PCM algorithm against the experimental results of Kuznik and Virgone [73] where strong agreement was observed between the experimental data and the numerical simulation for zone air temperature with roughly an average deviation of 3% for both PCM-integrated and non PCM-integrated models. In addition, Auzeby et al. [74] validated the simulation results of indoor air temperature of their building model with field measured data from a greenhouse and a maximum error of 2.6 ºC, mean error of 0.1 ºC, and standard deviation of 0.7 ºC were found. Moreover, Sage-Lauck et al. [75] validated their building energy model against measured data. Comparison of the observed room air temperature of the west unit of a house with the simulated room air temperature in a summer month showed 1.6 ºC and 1.0 ºC root mean squared error (RMSE) for hourly average zone temperature and daily maximum temperature, respectively. The disparities were considered to be due to uncertainties in occupants behavior or occupancy schedule.

In the present study, in all models the simulation time step was set to 1 minute and the node discretization of 3 was selected, otherwise inaccuracies may occur in simulation results [70].

2.4. Optimization

A generic optimization program (GenOpt v3.1.1) [76] was chosen because of its capabilities in solving optimization problems corresponding to the building energy performance, where parametric analysis is not feasible or efficient. GenOpt has gained increasing interest among researchers [47] for its flexibility to interface with any simulation program that calculates the objective function with no need to modify or recompile either program, taking into account that the simulation program reads its input from text files and writes its output to text files; such as EnergyPlus. The user can optionally select an optimization algorithm from GenOpt algorithm library, or even implement a custom algorithm. GenOpt has been developed to efficiently find the independent variables that yield better performance of physical systems. It performs optimization of a user-defined cost function such as, annual energy consumption, thermal comfort, etc. using various numerical optimization algorithms that could be chosen by the user. It can also find unknown parameters in a data-fitting process [77].

The cost function measures a quantity that should be minimized. Generally, the optimization problems addressed by GenOpt could be described as shown in (Eq. (3)):

$$\min_{x \in X} f(x) \qquad \text{(Eq. 3)}$$

where $f: X \rightarrow \mathbb{R}$ is the user-specified objective function, X is a user-specified constraint set for x, which consists of all possible design alternatives, and the cost function $f(\cdot)$ measures the system performance.

The optimization design parameters are the peak melting temperatures of the PCM drywalls incorporated into the building envelope, which are independent continuous variables and can take on any value on the real line (refer to Eq. 2)), box-constrained between lower and upper bounds as shown in (Eq. 4):

$$X \triangleq \left\{ x \in \mathbf{R}^n \,\middle|\, l^i \leq x^i \leq u^i, i \in \{1, \ldots, n\} \right\},$$

$$\text{where } -\infty \leq l^i < u^i \leq \infty \text{ for } i \in \{1, \ldots, n\}. \qquad \text{(Eq. 4)}$$

where $f: \mathbf{R}^n \rightarrow \mathbf{R}$ is the objective function, $x \in X \subset \mathbf{R}^n$ is the set of design parameters, X is the possible set for x, $l \in \mathbf{R}^n$ is the lower bound, and $u \in \mathbf{R}^n$ is the upper bound for design options.

Three different optimization scenarios were considered to optimize the energy performance of the apartment building enhanced with PCM drywalls. It can be seen that in three proposed scenarios the optimization is applied throughout the year and not only for cooling and heating seasons. In fact, in integrated passive designs, the building is influenced by the PCM technology all over the year, therefore, an optimization which exploits the highest annual energy benefits by applying this innovative technology should be considered. Otherwise, for example, in cooling period the PCM technology could be very energy-beneficial but in heating period, it might lead to adverse energy-related benefits. Accordingly, in the first scenario, the objective function was formulated to find an optimum PCM peak melting point to minimize only the annual cooling energy consumption (Eq. 5). In the second and third scenarios, the objective functions were formulated to reduce the annual heating (Eq. 6) and total annual (heating and cooling) energy consumption (Eq. 7), respectively. So that, for each climate zone these three scenarios were taken into account.

$$f_c(x) = Q_{cooling}(x) \quad \text{(Eq. 5)}$$

$$f_h(x) = Q_{heating}(x) \quad \text{(Eq. 6)}$$

$$f_{tot}(x) = Q_{total}(x) \quad \text{(Eq. 7)}$$

To reduce the risk of not achieving the optimum value and far from a minimizer of $f(\cdot)$, it is recommended to select different initial iterates and using the generalized pattern search (GPS) implementation of the Hooke-Jeeves algorithm [78,79]. This algorithm is a direct-search method that compares each trial solution with the best previous solution [81]. Further discussion can be found in Lewis et al. [81]. In general, these methods are efficient but can get trapped in local optima [50], however, using multiple initial points increases the opportunity of finding the global minimum if the objective function has several local minima such as the present study because different PCM melting points could be found as the optimum point. Additionally, it decreases the risk of not finding a minimum, if the cost function is not continuously differentiable, which might occur in case of using whole-building energy simulation tools such as EnergyPlus [79]. Accordingly, the Hooke-Jeeves algorithm with adaptive precision cost function evaluations using the GPS algorithm with multiple starting points was selected to minimize the cost functions in the present study [79]. Further details regarding the selection of optimization algorithm and the efficiency of different methods could be found in Wetter and Wright [80].

2.5. Köppen-Geiger climate classification

Herein, the updated Köppen-Geiger [82] main climates classification is used as a reference to the general climate of the regions of the world (Figure 4). This classification uses five letters to divide the world into five major climate regions, based on average annual precipitation, average monthly precipitation, and average monthly temperature which are A: equatorial, B: arid, C: warm temperate, D: snow, and E: polar. Additionally, the level of precipitation is defined as W: desert, S: steppe, f: fully humid, s: summer dry, w: winter dry, and m: monsoonal. Further details are provided regarding temperature as h: hot arid, k: cold arid, a: hot summer, b: warm summer, c: cool summer, d: extremely continental, and F: polar frost. In the present study, three different cities of each climate zone were selected. Table 4 presents the selected cities and their climate classification, geographical information as well as heating and cooling degree days.

Moreover, it should be added that Köppen-Geiger, despite of being one of the most frequently used climate classification, has some drawbacks. For instance, some factors such as wind characteristics, sunshine, precipitation intensity, amount of cloud cover, daily temperature extremes, and altitude above sea level are not taken into account. So that, while interpreting the simulation results in addition to using Köppen-Geiger scheme one should bear in mind these factors. For instance, generally global solar irradiance increases with increasing altitude above sea level. This increase is mainly due to a pronounced increase of direct irradiance, whereas for altitudes less than roughly 3000 m the diffuse irradiance is almost constant [83]. By the increase of global solar irradiance, the solar heat gains on the building surfaces increase which directly influences the energy balance of the whole system.

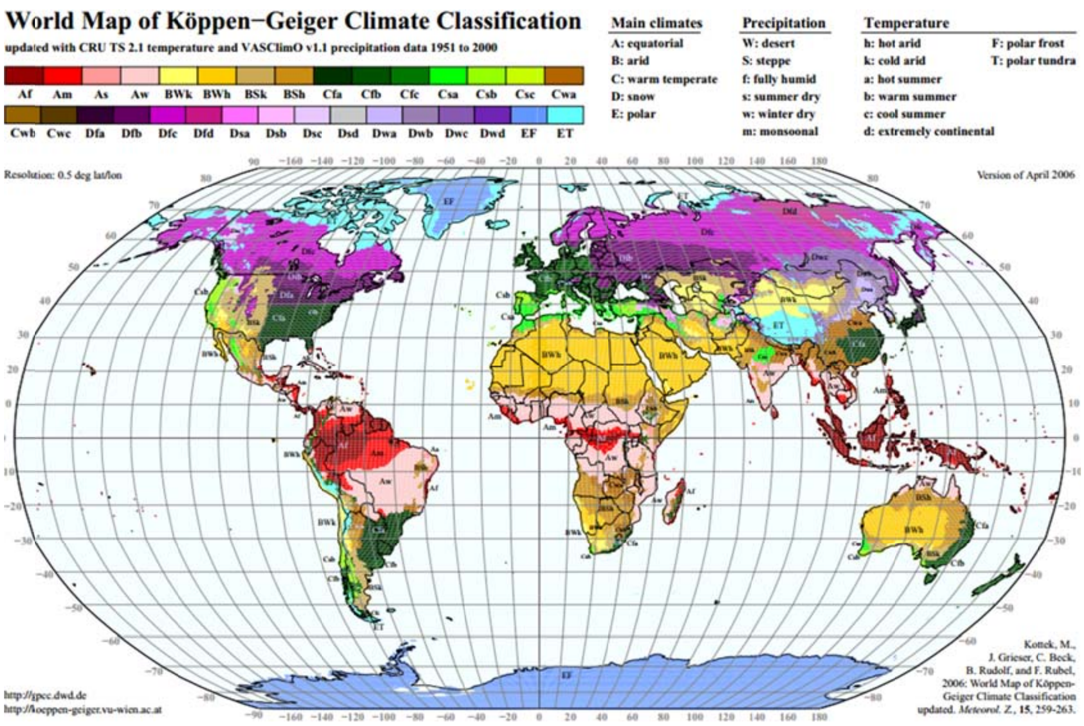

Figure 4.World Map of Köppen–Geiger climate classification [82].

475 Table 4. Selected locations and climate characteristics according to Köppen-Geiger classification [82].

Climate zone	City	Latitude	Longitude	Time zone (GMT)	Elevation [m]	CDD base 10 ºC	HDD base 18 ºC
Am	Manaus (Brazil)	S 3° 7'	W 60° 1'	-4.0	72	6487	0
	Freetown (Sierra Leone)	N 8° 29'	W 13° 14'	+0.0	26	6226	0
	Colombo (Sri Lanka)	N 6° 49'	E 79° 52'	+0.6	5	6299	0
Aw	Brasilia (Brazil)	S 15° 52'	W 47° 55'	-3.0	1061	4207	8
	Bangui (Central African)	N 4° 22'	E 18° 35'	+1.0	369	5965	6
	Kalkota (India)	N 22° 38'	E 88° 26'	+5.5	6	5931	18
As	Fortaleza (Brazil)	S 3° 46'	W 38° 31'	-3.0	25	6291	0
	Indore (India)	N 22° 43'	E 75° 48'	+5.5	567	5383	27
	Malindi (Kenya)	S 3° 13'	E 40° 5'	+3.0	23	5973	0
Af	Kuala Lumpur (Malaysia)	N 3° 7'	E 101° 33'	+8.0	22	6262	0
	Singapore	N 1° 22'	E 103° 58'	+8.0	16	6374	0
	Puerto Barrios (Guatemala)	N 15° 43'	W 88° 35'	-6.0	1	5690	0
BSk	Albuquerque (USA)	N 35° 2'	W 106° 37'	-7.0	1619	2157	2303
	Midland (USA)	N 31° 57'	W 102° 10'	-6.0	872	3043	1395
	Ceduna (Australia)	S 32° 7'	E 133° 41'	+9.5	16	2457	985
BSh	New Delhi (India)	N 28° 34'	E 77° 11'	+5.5	216	5363	278
	Dakar (Senegal)	N 14°41'	W 17° 26'	+0.0	22	5447	1
	Del Rio (USA)	N 29° 36'	W 100° 90'	-6.0	302	4427	697
BWh	Abu Dhabi (UAE)	N 24° 25'	E 54° 39'	+4.0	27	6254	24
	Jaisalmer (India)	N 26° 53'	E 70° 55'	+5.5	242	6032	136
	Phoenix (USA)	N 33° 25'	W 112° 1'	-7.0	339	4624	628
BWk	Calama (Chile)	S 22° 50'	W 68° 90'	-4.0	2312	2109	1919
	Las Vegas (USA)	N 36° 4'	W 115° 10'	-8.0	664	3680	1248
	Yumenzhen (China)	N 40° 16'	E 97° 1'	+8.0	1526	1363	4207
Cfa	Brisbane (Australia)	S 27° 22'	E 153° 6'	+10.0	5	3652	329
	Madrid (Spain)	N 40° 27'	W 3° 32'	+1.0	582	2057	1965
	Tokyo (Japan)	N 36° 10'	E 140° 25'	+9.0	35	1911	2311
Cfb	Berlin (Germany)	N 52° 28'	E 13° 23'	+1.0	49	1125	3156
	Johannesburg (South Africa)	S 26° 7'	E 28° 13'	+2.0	1700	2216	1052
	Paris (France)	N 48° 43'	E 2° 24'	+1.0	96	1209	2644
Csb	Antofagasta (Chile)	S 23° 25'	W 70° 25'	-4.0	40	2557	598
	Ankara (Turkey)	N 40° 7'	E 32° 58'	+2.0	950	1338	3307
	San Francisco (USA)	N 37° 37'	W 122° 24'	-8.0	2	1436	1557
Csa	Tehran (Iran)	N 35° 24'	E 51° 11'	+3.0	1190	3230	577
	Seville (Spain)	N 37° 25'	W 5° 54'	+1.0	31	3128	916
	Cagliari (Italy)	N 39° 15'	E 9° 3'	+1.0	18	2454	1207
Cwa	Rangpur (Bangladesh)	N 25° 43'	E 89° 13'	+6.0	34	5259	71
	Hong Kong (China)	N 22° 19'	E 114° 10'	+8.0	65	4782	202
	Ankang (China)	N 32° 43'	E 109° 1'	+8.0	291	2647	1745
Cwb	Huili (China)	N 26° 38'	E 102° 15'	+8.0	1787	2194	1284
	Jiulong (China)	N 29° 0'	E 101° 30'	+8.0	2987	697	3284
	Addis Ababa (Ethiopia)	N 8° 58'	E 38° 47'	+3.0	2355	2245	705
Dfa	Chicago (USA)	N 41° 46'	W 87° 45'	-6.0	186	1964	3106
	Omaha (USA)	N 41° 22'	W 96° 31'	-6.0	404	1970	3294

	Cleveland (USA)	N 41° 24'	W 81° 50'	-5.0	245	1607	3255
Dfb	Montreal (Canada)	N 45° 28'	W 73° 45'	-5.0	36	1185	4493
	Moscow (Russia)	N 55° 45'	E 37° 37'	+3.0	156	862	4655
	Stockholm (Sweden)	N 59° 39'	E 17° 57'	+1.0	61	683	4239
Dwa	Beijing (China)	N 39° 47'	E 116° 28'	+8.0	32	2321	2750
	Incheon (South Korea)	N 37° 29'	E 126° 38'	+9.0	45	2248	2681
	Pyongyang (North Korea)	N 39° 03'	E 125° 76'	+8.50	38	2189	3114
Dfc	Yellowknife (Canada)	N 62° 28'	W 114° 26'	-7.0	206	487	8257
	Anchorage (USA)	N 61° 10'	W 150° 1'	-9.0	35	383	5611
	Kiruna (Sweden)	N 67° 49'	E 20° 19'	+1.0	452	140	6967
Dwb	Linjiang (China)	N 41º 81'	N 126º 91'	+8.0	341	1454	4969
	Linxi (China)	N 43° 35'	E 118° 4'	+8.0	800	1167	5033
	Pingliang (China)	N 35° 32'	E 106° 40'	+8.0	1347	1332	3540

*Note: GMT, Greenwich Mean Time; CDD, cooling degree days; HDD, heating degree days.

3. Results

3.1. Impact of PCM on the annual cooling

Table 5 shows the annual cooling energy performance of the apartment building enhanced with PCM under different climate classifications. Generally, it can be seen that, under almost all climate conditions, the optimum PCM peak melting temperature to enhance the cooling energy performance ranges from 24ºC (melting range of 22ºC-26ºC) to 26ºC (melting range of 24ºC-28ºC). This could be justified since the PCM required high melting temperature to be able to be charged during night time. However, in general, according to simulation results it can be said that the utilization of PCM is not very feasible in equatorial climates (Köppen-Geiger classification A) with some exceptions such as Brasilia and Indore. For example, the cooling energy consumption increased by 4% (1924 kWh) and 9% (3984 kWh) in Freetown and Manaus, respectively, with tropical monsoon weather conditions. Similarly, very limited cooling energy savings were achieved in other equatorial climate zones such as Fortaleza and Singapore with 0.23% (117 kWh) and 0.43% (213 kWh) of cooling energy savings, respectively. However, some researchers [44] showed that, higher savings could be achieved in Singapore by varying the location of PCM in the building envelope and using PCM with higher melting point range. Because when the PCM is installed on the outer surface of exterior walls the stored heat can be dissipated easier at night time, so that it does not adversely influence the occupant's thermal comfort.

To have a closer view of cooling energy savings in equatorial climate zone, a more detailed analysis could be presented comparing two different cities of Brasilia and Singapore. In Brasilia high cooling savings were recorded (17% or 1373 kWh) while the cooling savings in Singapore were very limited. The cooling energy consumption without PCM technology in Brasilia and Singapore were 7857 kWh and 50000 kWh, respectively. Afterwards, by adding the PCM technology cooling savings of 17% (1373 kWh) and 0.43% (213 kWh) were achieved. It can be seen that there is a stark contrast between these two cities in terms of cooling energy savings, despite of being in the same climate category. As mentioned earlier in section 2.5, there are several possible explanations for these results. First of all, Brasilia has an altitude of 1061m in comparison to 165m in Singapore which influences the solar radiation, sky cover, and wind characteristics. For example, in Brasilia the monthly average direct normal radiation is about 266 Wh/m^2 in comparison to 85 Wh/m^2 in Singapore. In addition, the monthly average sky cover percentage in Brasilia is about 56% compared to 87% in Singapore. Further on, the ratio of average monthly relative humidity in Singapore (82%) is higher than Brasilia (70%) which affects the energy consumption. It should be considered that the HVAC system has humidification and dehumidification control so that, when the relative humidity level is out of determined comfort level, a considerable amount of energy is consumed to decrease these level. Moreover, in Brasilia the monthly average wind speed is about 2.5 m/s compared to 1.5 m/s in Singapore. The wind speed influences the external convective heat transfer coefficient which has a linear impact with heat transfer. So that, the higher wind speed improves the charging of PCM with cool night time temperature.

Under arid (Köppen-Geiger classification B) weather condition, the use of PCM yielded high cooling energy savings from roughly 300 kWh to 1000 kWh, with higher savings in lands with higher elevations from sea level. For instance, in Ceduna, 29% (769 kWh) of cooling savings were achieved by using optimum PCM peak melting point of 25 ºC. In Phoenix, 3% (850 kWh) of cooling energy consumption saved by applying PCM melting at 26 ºC, which is consistent with results of Kośny et al. [84]. In Calama about 50% (325 kWh) of cooling saved which is in agreement with findings of Marin et al. [85].

In warm temperate climates (Köppen-Geiger classification C), the PCM melting at 26ºC (24ºC-28ºC melting range) yielded higher cooling energy savings in almost all cities except Hong Kong with lower cooling energy savings. Further on, in some cities no cooling energy was required such as Addis Abeba. For example, for buildings located in Madrid, Johannesburg, Ankara, and Cagliari cooling energy savings of 8% (527 kWh), 67% (721 kWh), 33% (907 kWh), and 10% (408 kWh) were obtained, respectively. This is reasonable because passive PCM technology could be very effective in terms of cooling energy improvements. However the cooling savings in Hong Kong was not considerable and were limited to only 1% (271 kWh). Similarly, Mi et al. [86] concluded that in Hong Kong the application of PCM melting at

27ºC could not be economically feasible because the PCM could not be effectively charged and discharged due to outdoor temperature constraints.

To have a better understanding, the results of Cagliari and Hong Kong could be compared. In Cagliari and Hong Kong the cooling energy consumptions without using the PCM passive system were 4140 kWh and 24775 kWh, respectively. By PCM inclusion into the building envelope savings of 408 kWh in Cagliari and 271 kWh in Hong Kong were achieved. A reason for this difference higher amount of direct normal solar radiation (215 Wh/m^2 and 180 Wh/m^2 monthly averages in Cagliari and Hong Kong) and also higher monthly average wind speed in Cagliari 4 m/s compared to 3 m/s in Hong Kong.

Further on, the application of optimized PCM in cold climates (Köppen-Geiger classification D) resulted in considerable cooling energy savings. For instance, in Chicago, Montreal, and Pingliang the cooling energy consumption without PCM incorporation were obtained as 6632 kWh, 1086 kWh, and 1419 kWh. Adding passive PCM led to cooling energy savings of 8% (545 kWh) in Chicago, 28% (308 kWh) in Montreal, and 33% (467 kWh) in Pingliang with some exceptions such as Stockholm, Yellowknife, and Anchorage. One should bear in mind that the high percentage of cooling savings in these cities does not signify a high proportion of savings compared to total annual cooling and heating savings. Therefore, one should refer also to energy savings in kilowatt-hour. These results therefore need to be interpreted with caution.

For instance, the cooling energy consumptions in Stockholm, Yellowknife, Anchorage, and Antofagasta without PCM enhancement were about 35 kWh, 24 kWh, 10 kWh, and 26 kWh, respectively. It can be seen that the cooling requirements in these regions are negligible; and adding PCM, despite of reducing a major portion of the cooling consumption in above-mentioned cities, is still unfeasible because a great part of the energy consumption in these regions come from heating energy needs.

Table 5. Optimum PCM peak melting temperature for only annual cooling energy consumption.

Climate zones	Cities	Melting point for cooling [ºC]	Cooling savings		Climate zones	Cities	Melting point for cooling [ºC]	Cooling savings	
			[kWh]	[%]				[kWh]	[%]
	Manaus	26.00	-3984	-8.8%		Antofagasta	24.94	21	82.8%
Am	Freetown	26.00	-1924	-4.3%	Csb	Ankara	25.43	907	32.9%
	Colombo	22.44	-32	-0.1%		San Francisco	-	-	-
	Brasilia	25.88	1373	17.5%		Tehran	26.00	503	2.6%
Aw	Bangui	25.94	589	1.5%	Csa	Seville	26.00	625	4.9%
	Kolkata	26.00	684	1.4%		Cagliari	26.00	408	9.9%
	Fortaleza	24.13	113	0.23%		Rangpur	25.50	549	1.4%
As	Indore	26.00	1020	3.3%	Cwa	Hong Kong	25.38	271	1.1%
	Malindi	25.81	157	0.4%		Ankang	25.75	440	3.2%
	Kuala Lumpur	25.38	171	0.36%		Huili	25.38	470	45.8%
Af	Singapore	25.50	213	0.43%	Cwb	Jiulong	-	-	-
	Puerto Barrios	25.63	3054	8.00%		Addis Abeba	-	-	-
	Albuquerque	25.94	497	7.8%		Chicago	25.63	545	8.2%
BsK	Midland	25.63	575	4.8%	Dfa	Omaha	25.81	523	8.1%
	Ceduna	25.13	769	28.5%		Cleveland	25.38	449	21.4%
	New Delhi	25.38	592	1.3%		Montreal	25.38	308	28.4%
BSh	Dakar	25.50	561	1.9%	Dfb	Moscow	24.94	326	37.7%
	Del Rio	25.88	572	2.3%		Stockholm	24.56	27	78.2%
	Abu Dhabi	26.00	970	1.8%		Beijing	25.38	379	4.2%
BWh	Jaisalmer	25.94	760	1.4%	Dwa	Incheon	25.63	361	8.4%
	Phoenix	26.00	850	2.7%		Pyongyang	25.88	339	5.3%
	Calama	24.88	325	56.7%		Yellowknife	24.13	22	90.3%
BWk	Las Vegas	26.00	679	3.0%	Dfc	Anchorage	24.13	9	95.4%
	Yumenzhen	25.25	396	37.4%		Kiruna	-	-	-
	Brisbane	25.19	612	8.1%		Linjiang	26.00	398	11.9%
Cfa	Madrid	25.75	527	7.6%	Dwb	Linxi	25.38	485	28.6%
	Tokyo	25.31	537	13.5%		Pingliang	25.31	467	32.9%
	Berlin	24.63	253	47.7%	---	---	---	---	---
Cfb	Johannesburg	24.88	721	67.0%	---	---	---	---	---
	Paris	25.13	173	59.3%	---	---	---	---	---

3.2. Impact of PCM on the annual heating

Table 6 shows the annual heating energy performance of the apartment building enhanced with passive PCM system under different climate conditions. It is apparent from the results that in equatorial climates (Köppen-Geiger classification A) such as Freetown, Bangui, and Singapore no heating was required. Additionally, in other cities such as Brasilia and Indore the heating savings were negligible.

The application of passive PCM system in residential buildings to enhance the cooling energy performance has been investigated by many researchers [38], nevertheless, less attention has been paid to the use of PCM for improving the heating energy performance [33]. It should be taken into account that by numerical optimization considerable heating savings can be achieved [87]. In the present study, it can be seen that by proper optimization-based design techniques high heating energy savings could be achieved by integrating the PCM in the building envelope. Table 6 shows that the optimization of PCM melting temperature in arid and temperate climates (Köppen-Geiger classifications B and C) led to high heating energy savings except in some cities with negligible or no heating savings such as New Delhi, Abu Dhabi, Rangpur, and Dakar. The possible explanation for these results is that in these cities the cooling requirements are much higher than heating requirement. For example, the heating energy consumptions without PCM inclusion in New Delhi, Abu Dhabi, and Rangpur were achieved as 811, 25, and 28 kWh, respectively.

On the other hand, using PCM wallboards with optimized melting temperature of 20ºC could achieve important heating energy savings of 4% (1187 kWh) in Midland, 8% (810 kWh) in Del Rio, 3% (509 kWh) in Las Vegas, 21% (2736 kWh) in Johannesburg, 2.5% (686 kWh) in Tehran, and 4.8% (496 kWh) in Seville. To have a closer view of energy savings, it can be referred to energy consumption and geographical characteristics of Tehran and Johannesburg, both of which with higher than 1000m elevation from sea level. In both of these cities high amount of energy is required for heating purposes. With no PCM technology 27240 kWh and 12640 kWh of heating energy consumptions were obtained in Tehran and Johannesburg, subsequently. Winter average direct normal radiation in Tehran is about 300 Wh/m^2 and in Johannesburg about 550 Wh/m^2 which helps the PCM to melt in sunshine hours and to solidify when the outdoor temperature falls down during cold nights of winter season. In addition, in such regions with high elevation there is relatively medium to high wind speed which improves the charging and discharging cycle of the passive system.

It has been seen that in many cities PCM melting at about 20ºC was the optimum melting temperature to increase heating energy performance. However, in some cities such as Yumenzhen and Berlin the optimum PCM melting temperatures were obtained as 26ºC and 24ºC, respectively. This discrepancy may be due to elevation, solar radiation, and wind profile as mentioned before.

In heating dominant lands or cold regions with high heating energy consumption (Köppen-Geiger classification D), a considerable amount of heating energy is required to provide indoor comfort temperature for occupants. The results show notable heating savings by using optimized PCM passive technology in cold climates. For example, by applying PCM melting at about 20ºC in Omaha, Kiruna, and Pingliang heating savings of 1786 kWh, 3045 kWh, and 2242 kWh were achieved, respectively, with some exceptions in Montreal, Beijing, and Linxi with optimum PCM melting from 25ºC to 26ºC, which could be due to other climatic and geographical conditions as discussed in previous sections.

Table 6. Optimum PCM peak melting temperature for only annual heating energy consumption.

Climate zones	Cities	Melting point for heating [ºC]	Heating savings		Climate zones	Cities	Melting point for heating [ºC]	Heating savings	
			[kWh]	[%]				[kWh]	[%]
Am	Manaus	-	-	-	Csb	Antofagasta	20.00	128	4.9%
	Freetown	-	-	-		Ankara	20.00	1850	2.0%
	Colombo	-	-	-		San Francisco	20.06	760	3.8%
Aw	Brasilia	23.13	4	30.5%	Csa	Tehran	20.00	686	2.5%
	Bangui	-	-	-		Seville	20.00	496	4.8%
	Kolkata	22.00	2	20.4%		Cagliari	20.00	376	1.7%
As	Fortaleza	-	-	-	Cwa	Rangpur	22.50	7	23.3%
	Indore	24.13	4	16.8%		Hong Kong	20.13	280	22.6%
	Malindi	-	-	-		Ankang	20.00	632	2.1%
Af	Kuala Lumpur	-	-	-	Cwb	Huili	20.00	786	4.3%
	Singapore	-	-	-		Jiulong	20.00	1705	2.2%
	Puerto Barrios	-	-	-		Addis Abeba	21.00	416	29.0%
BsK	Albuquerque	20.00	1269	2.6%	Dfa	Chicago	20.00	1365	1.2%
	Midland	20.00	1187	3.9%		Omaha	20.00	1786	1.4%
	Ceduna	20.00	521	4.8%		Cleveland	20.00	1742	1.4%
BSh	New Delhi	20.00	84	10.3%	Dfb	Montreal	25.44	3258	1.7%
	Dakar	-	-	-		Moscow	22.13	1639	0.9%
	Del Rio	20.38	810	8.3%		Stockholm	21.50	5722	3.3%
BWh	Abu Dhabi	24.00	6	25.1%	Dwa	Beijing	25.63	2773	3.2%
	Jaisalmer	20.56	55	29.1%		Incheon	20.00	851	1.0%
	Phoenix	20.00	445	6.7%		Pyongyang	20.00	1412	1.4%
BWk	Calama	20.00	128	3.5%	Dfc	Yellowknife	23.75	5515	1.3%
	Las Vegas	20.56	509	3.1%		Anchorage	23.63	5701	2.5%
	Yumenzhen	26.00	4845	3.1%		Kiruna	20.19	3045	1.0%
Cfa	Brisbane	20.00	151	7.7%	Dwb	Linjiang	20.00	1657	0.9%
	Madrid	20.00	974	2.8%		Linxi	26.00	3428	1.7%
	Tokyo	20.00	743	1.3%		Pingliang	20.00	2242	2.1%
Cfb	Berlin	24.38	1803	1.5%	---	---	---	---	---
	Johannesburg	20.31	2736	21.6%	---	---	---	---	---
	Paris	24.06	1418	1.7%	---	---	---	---	---

3.3. Impact of PCM on the annual total heating and cooling

Table 7 presents the optimization results of PCM melting temperature for the annual total heating and cooling energy consumption. It can be seen that the optimum peak melting temperature of the PCM highly depends on the climate condition of each specific city, and in many cases the altitude of the region.

Moreover, in general, it can be said that in cooling dominant climates (Köppen-Geiger classifications A and B) the optimum PCM peak melting temperature is closer to the maximum of 26ºC (melting range of 24ºC-28ºC), whereas in heating dominant climates (C and D) is closer to the minimum of 20ºC (melting range of 18ºC-22ºC) with some exceptions such as Anchorage (23ºC), Paris (24ºC), and Chicago (25ºC). Further on, it can be seen from Table 7 that in equatorial-monsoonal climate zones (Am) the application of PCM is not feasible and it causes the increase of the annual energy consumption.

Table 7. Optimum PCM peak melting temperature for total annual cooling and heating energy consumption.

Climate zones	Cities	Melting point for heating & cooling [ºC]	Total heating & cooling savings		Climate zones	Cities	Melting point for heating & cooling [ºC]	Total heating & cooling savings	
			[kWh]	[%]				[kWh]	[%]
Am	Manaus	26.00	-3984	-9.0%	Csb	Antofagasta	20.00	133	5.1%
	Freetown	26.00	-1924	-4.3%		Ankara	20.00	1813	2.0%
	Colombo	22.44	-32	-0.1%		San Francisco	20.06	760	3.8%
Aw	Brasilia	25.88	1376	17.5%	Csa	Tehran	20.00	922	2.0%
	Bangui	25.94	589	1.5%		Seville	26.00	811	3.5%
	Kolkata	26.00	685	1.4%		Cagliari	24.44	450	1.7%
As	Fortaleza	24.13	113	0.2%	Cwa	Rangpur	25.50	554	1.4%
	Indore	26.00	1023	3.3%		Hong Kong	20.13	343	1.3%
	Malindi	25.81	157	0.4%		Ankang	25.19	1013	2.3%
Af	Kuala Lumpur	25.38	171	0.4%	Cwb	Huili	20.00	836	4.3%
	Singapore	25.50	213	0.4%		Jiulong	20.00	1705	2.2%
	Puerto Barrios	25.63	3054	8.0%		Addis Abeba	26.00	166	12.0%
BsK	Albuquerque	20.00	1381	2.5%	Dfa	Chicago	25.13	1704	1.4%
	Midland	20.00	1300	3.0%		Omaha	26.00	1952	1.5%
	Ceduna	25.06	987	7.3%		Cleveland	25.63	3492	2.8%
BSh	New Delhi	25.38	619	1.4%	Dfb	Montreal	25.44	3565	1.9%
	Dakar	25.50	561	1.9%		Moscow	24.31	2117	1.2%
	Del Rio	25.63	825	2.4%		Stockholm	21.50	5741	3.3%
BWh	Abu Dhabi	26.00	975	1.8%	Dwa	Beijing	25.63	3099	3.3%
	Jaisalmer	25.94	770	1.4%		Incheon	20.00	883	1.0%
	Phoenix	26.00	1018	2.7%		Pyongyang	25.63	2892	2.6%
BWk	Calama	25.63	317	7.5%	Dfc	Yellowknife	23.75	5537	1.3%
	Las Vegas	26.00	1018	2.6%		Anchorage	23.94	5709	2.5%
	Yumenzhen	26.00	5213	3.3%		Kiruna	20.19	3045	1.0%
Cfa	Brisbane	25.19	656	6.9%	Dwb	Linjiang	25.00	1848	1.0%
	Madrid	20.00	1093	2.6%		Linxi	26.00	3865	1.9%
	Tokyo	20.00	791	1.2%		Pingliang	20.00	2292	2.1%
Cfb	Berlin	24.38	2054	1.7%	---	---	---	---	---
	Johannesburg	25.56	4000	22.7%	---	---	---	---	---
	Paris	24.06	1564	1.9%	---	---	---	---	---

Furthermore, to have a clearer view of the PCM melting point selection in different climatic zones, the energy consumption curves as function of PCM peak melting temperatures (18ºC-27ºC) were studied for three different cities (Figures 5-7). In each figure three different measures of cooling, heating, and annual total heating and cooling energy consumptions as function of PCM melting temperature are illustrated. Figure 5 shows the cooling, heating and total energy consumption in heating predominant climate of Stockholm. It can be seen that the best PCM melting temperature for cooling is 24.56 ºC, while for heating and annual total heating and cooling the PCM with 21.50ºC leads to higher savings. However, the interesting point is that the annual total energy consumption curve is very similar to the heating energy consumption trend. This could be justified because in cold climate of Stockholm higher energy is required for heating purposes, so that, an ideal PCM could be a PCM with lower melting temperature which can be effectively melted and solidified in cold seasons by solar heat. Hence, it can be seen that for the total annual heating and cooling energy consumption a PCM melting at about 21 ºC is the optimum solution for energy saving.

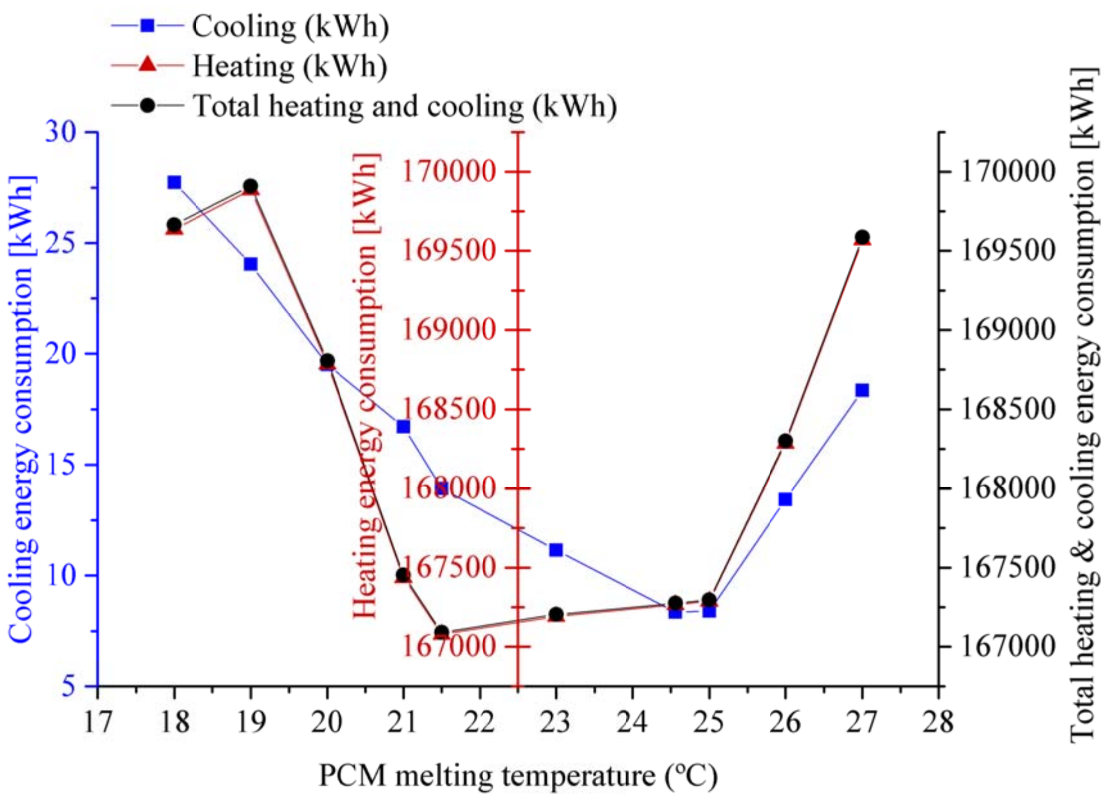

Figure 5. Energy consumption curves as function of PCM melting temperature in Stockholm.

On the other hand, Figure 6 shows the energy performance curves as function of PCM temperature under cooling dominant climate of Brisbane. This means that throughout the year higher energy is required to provide cooling to maintain the indoor air condition comfortable. In this climate PCM melting at about 25ºC gives the highest cooling savings, nevertheless, PCM with 20ºC of melting point achieves higher energy savings for cooling period, but, when the annual total energy performance is considered PCM melting at about 25ºC achieves the highest energy performance. This is an important issue which is not clearly addressed in the current literature on the passive PCM design for building applications. In Figure 6 in can be seen that selecting PCM melting at 20ºC reduces the heating energy consumption to 1870 kWh. In addition, for cooling and annual total heating and cooling energy performance selecting PCM with 25 ºC peak melting temperature decreases the energy consumption to 6950 kWh and 8950 kWh, respectively. The cooling energy requirement is approximately 80% of the total annual energy consumption, and four times higher than the heating energy requirement, for this sake, it is more energy-beneficial to use a PCM with higher peak melting temperature (25 ºC in this specific climate) suitable to maintain the indoor temperature comfortable for cooling seasons.

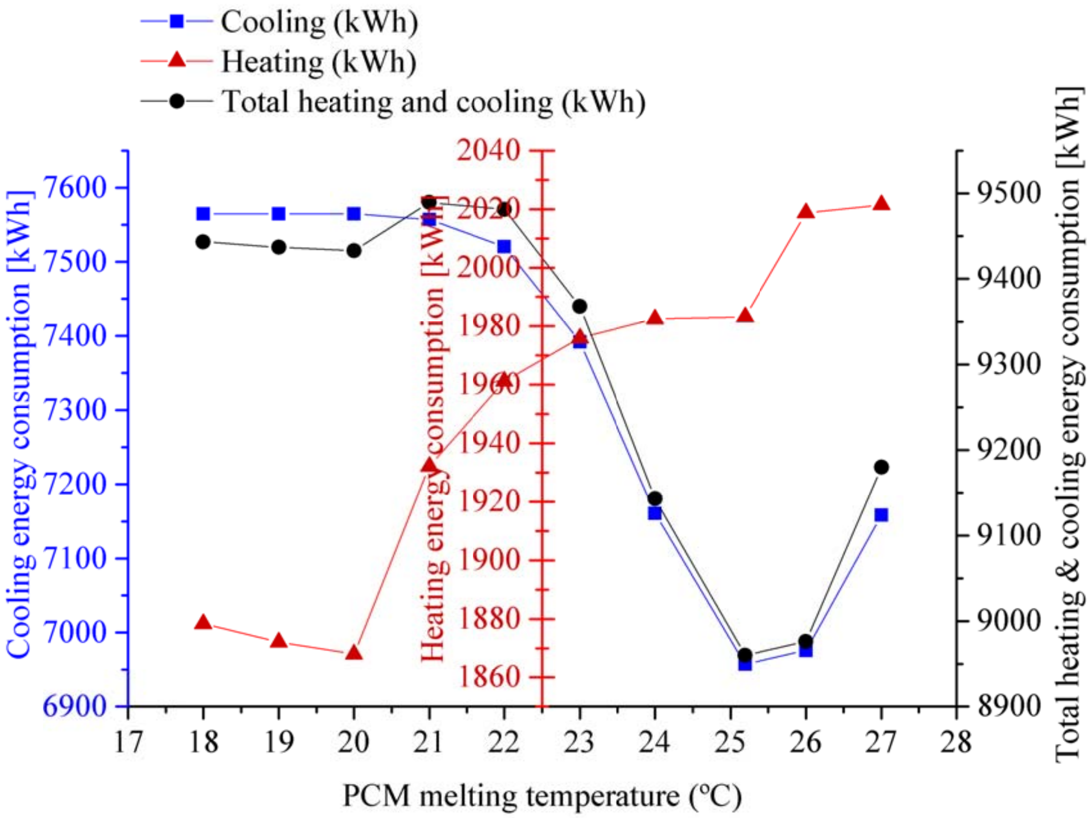

Figure 6. Energy consumption curves as function of PCM melting temperature in Brisbane.

Similarly, in Figure 7 where the energy consumption curves of Seville, Spain are shown. To better understand the energy benefits due to optimization, special attention should be paid to energy consumption curves in Figure 7. It can be seen that, if only heating energy saving is considered, the optimum PCM melting temperature is 18 ºC with heating consumption of about 16200 kWh, whereas for cooling consumption, the PCM melting at 27 ºC achieved the lowest energy consumption (22250 kWh). More interestingly, when the annual total heating and cooling energy consumption was considered, PCM melting at about 26 ºC resulted in annual total energy consumption of 38800 kWh with improved energy savings of about 350 kWh, when compared to the sum of energy savings for only heating and only cooling.

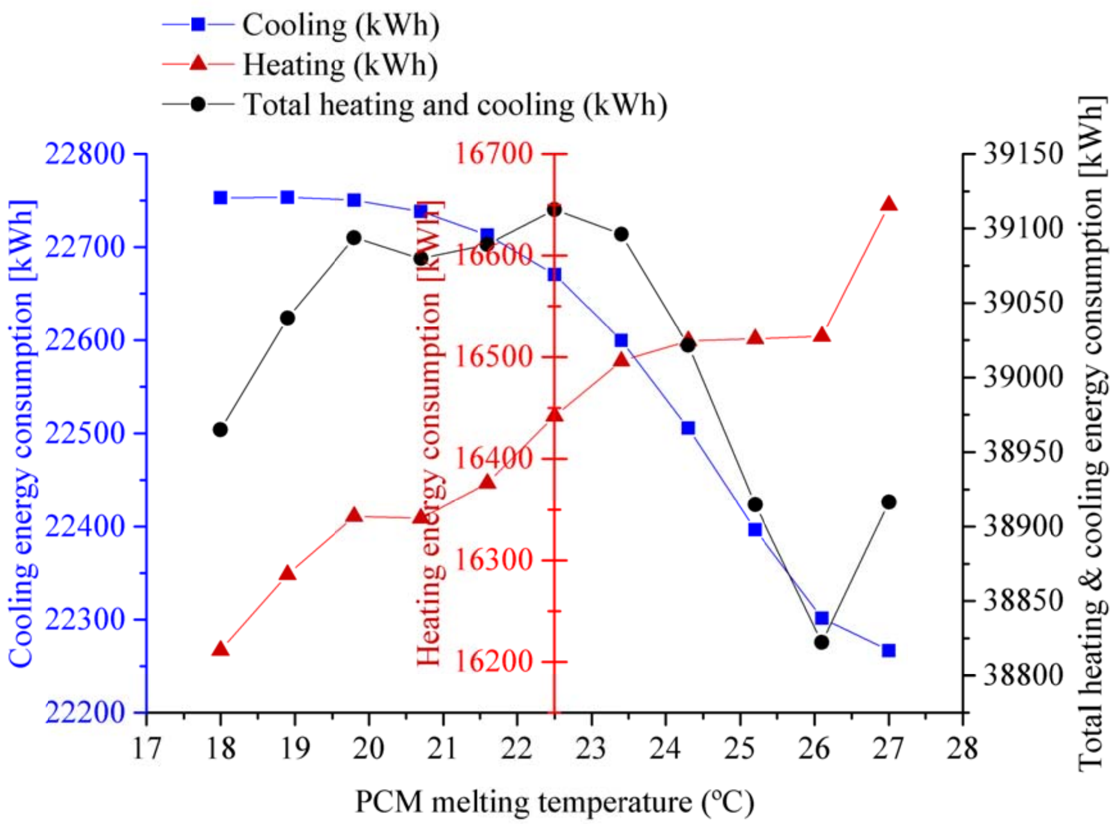

Figure 7. Energy consumption curves as function of PCM melting temperature in Seville.

In general, the interesting correlations between the energy consumption curves and the PCM melting point in Figures 5, 6, and 7 show that the optimum PCM melting temperature in a specific climate has strong correlation with heating and cooling energy requirements, but not limited to these factors. Figure 8 shows the worldwide distribution of optimum PCM melting temperature in different climates according to Köppen-Geiger classification. For example, it can be seen that different optimum PCM peak melting temperatures were obtained to enhance the annual total heating and cooling energy performance in Madrid and Seville, both of which with warm temperate classification (C). This could be because of other influencing factors such as the altitude, the humidity ratio, intensity of solar irradiance on the exterior surfaces, and wind characteristics of these regions. Additionally, it can be perceived that in high latitude regions such as Stockholm, a high amount of energy consumption for heating could be saved, however, an important issue that should be taken into account in designing PCM-enhanced passive buildings, is the proper optimization of PCM melting temperature considering the overall annual benefits. Also, another achievement that is noteworthy is that the PCM-enhanced gypsum technology can lead to notable energy savings in many regions in the world, for both heating and cooling dominant climate zones.

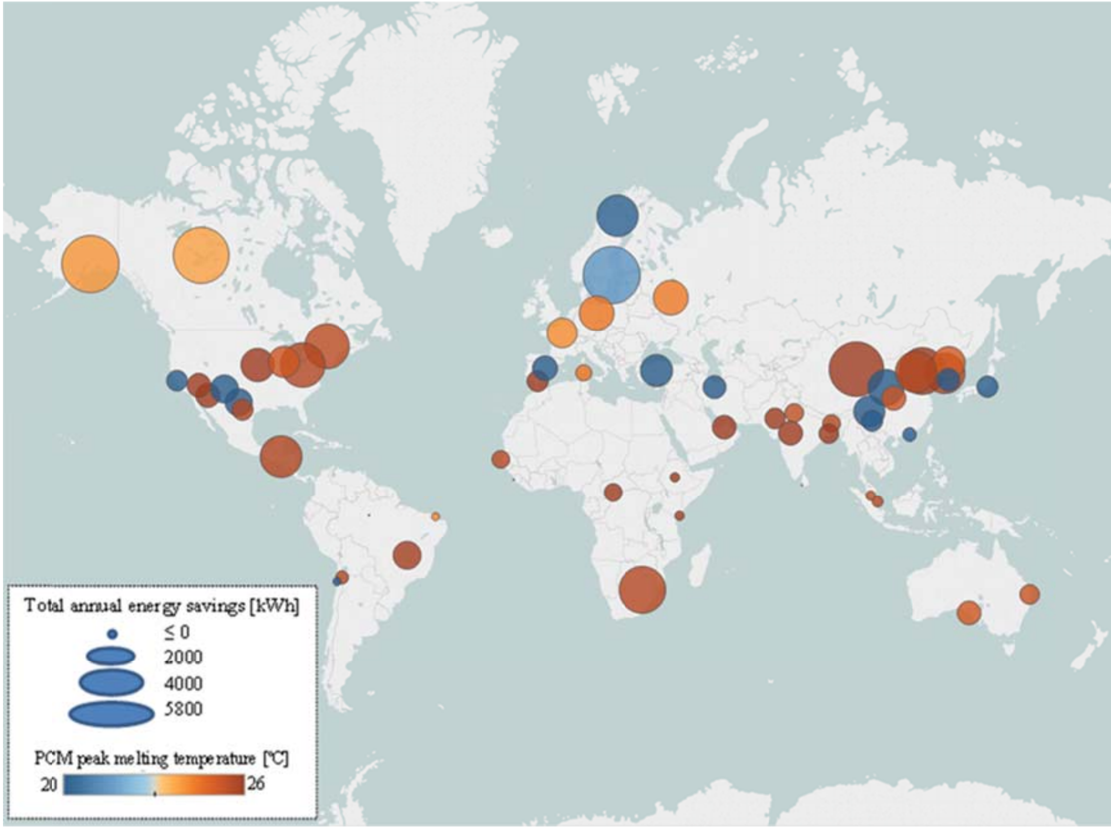

Figure 8. Global energy savings due to use of PCM passive system in building envelopes.

What is interesting in the presented results is that, apart from the climate classification other critical climatic factors such as elevation from sea level, solar irradiance and sunshine duration, wind profile (speed and direction), and sky cover highly influence the effectiveness of the passive PCM technology which should be taken into account when designing passive buildings otherwise the benefits of such innovative technologies could be partially exploited. Further on, it should be added that, savings presented in this paper may vary depending on the building type, HVAC schedule, internal gains, the PCM location in the envelope, and more importantly the amount and type of PCM.

As an example, for three cities of Stockholm, Brisbane, and Seville the influence of increasing the PCM quantity (by increasing the wallboard thickness) on the annual energy performance and the optimum PCM melting temperature was studied and they are presented in Table 8.

Table 8. The influence of PCM quantity on the annual total energy performance and optimum PCM melting temperature.

City	PCM thickness [m]	Optimum peak melting [ºC]	Annual energy consumption with PCM [kWh]	Annual energy consumption without PCM [kWh]	Savings [kWh]	Savings [%]
Stockholm	0.0125	21	167072	172813	5741	3.32
	0.025	19	168989		3824	2.21
Brisbane	0.0125	25	8838	9493	655	6.90
	0.025	25	8532		961	10.12
Seville	0.0125	26	22204	23015	811	3.52
	0.025	20	21686		1329	5.77

It can be derived from Table 8 that in heating-dominant climate such as Stockholm the increase of PCM layer thickness reduces the optimum PCM peak melting temperature from 21ºC to 19ºC, and has an adverse effect on the annual energy savings. It can be seen that by increasing the PCM layer thickness the total annual energy savings decreases from 5741 kWh to 3824 kWh. A possible explanation for this is that a major part of the energy consumption comes from heating, thus, increasing the amount of PCM decreases the probability of an effective charging and discharging cycle of PCM. Therefore, it takes longer for PCM to be melted during sunshine hours; this is why by increasing the amount of PCM the optimum peak melting temperature decreases. In Brisbane, increasing the amount PCM by doubling the thickness of PCM gypsum board increased the annual energy savings from 6.9% to about 10%, nevertheless, the optimum PCM melting temperature did not change. This may explain the relatively good correlation between cooling savings and the amount of PCM which is consistent with previous findings [44]. However, it should be taken into account that in Brisbane about 80% of the annual energy is consumed for cooling purposes, based on the reference model energy consumption. By looking at the results of Seville, first, it can be seen that increasing the PCM quantity improves the annual energy savings from 3.5% to 5.7% that could have been expected since there is high cooling requirements in this climate. Secondly, the increase of PCM quantity reduces the optimum PCM peak melting temperature from 26ºC to 20ºC. The reason for this is because of considerable heating requirements in Seville. As explained before, when the PCM amount increases its charging and discharging cycle becomes more critical in heating season making PCM with lower peak melting point (20ºC) more appropriate.

4. Conclusions

In the present paper a simulation-based single-objective numerical optimization is presented to define the optimum PCM melting temperature of a wallboard integrated into a residential building envelope under a wide-range climate zone classifications based on Köppen-Geiger. An innovative continuous enthalpy-temperature (h-T) function was integrated to the optimization pre-processing step to find out the optimum PCM peak melting temperature iteratively. Simulation-based optimizations were carried out to optimize the PCM melting temperature to enhance the cooling, the heating, and the annual total heating and cooling energy performance.

This study has shown that the proper selection of PCM-enhanced gypsum technology as integrated passive system into the building envelopes can lead to notable energy savings in many regions in the world, for both heating and cooling dominant climates. Also, the present study has found that, generally, in cooling dominant climates (climates with high CDD) PCM melting at about 26 ºC (with melting range of 24 ºC-28 ºC) leads to higher energy savings such as Seville, while, in heating dominant climates (climates with high HDD) the best melting point for the PCM is close to 20 ºC (with melting range of 18 ºC-22 ºC) such as Stockholm. Furthermore, in climates with both heating and cooling energy demands (climates with high HDD and CDD) the optimum PCM melting point could be between the maximum and minimum peak melting temperatures such as Seville. Moreover, this research has shown that in almost all high-altitude regions considerable energy savings due to the use of PCM could be obtained. Also, when designing a passive building with PCM technology not only the climate classification should be considered, but also other geographical and climatic factors such as elevation from sea level, solar irradiance, and wind profile should be taken into account. The present study has gone some way towards enhancing our understanding of using and implementing the PCM-enhanced gypsum board technology under different climate conditions.

Acknowledgments

The work is partially funded by the Spanish government (ENE2015-64117-C5-1-R (MINECO/FEDER) and ENE2015-64117-C5-3-R (MINECO/FEDER)). The authors would like to thank the Catalan Government for the quality accreditation given to their research group GREA (2014 SGR 123). GREA is certified agent TECNIO in the category of technology developers from the Government of Catalonia. This project has received funding from the European Commission Seventh Framework Program (FP/2007-2013) under Grant agreement Nº PIRSES-GA-2013-610692 (INNOSTORAGE) and from the European Union's Horizon 2020 research and innovation program under grant agreement No 657466 (INPATH-TES). Alvaro de Gracia would like to thank Ministerio de Economia y Competitividad de España for Grant Juan de la Cierva, FJCI-2014-19940.

References

[1] S.B. Sadineni, S. Madala, R.F. Boehm, Passive building energy savings: A review of building envelope components, Renew. Sustain. Energy Rev. 15 (2011) 3617–3631.

[2] International Energy Agency, Technology Roadmap:Energy efficient building envelopes, Oecd. (2013).

[3] International Energy Agency, Energy Technology Perspectives 2012 Pathways to a Clean Energy System, 2012.

[4] H. Akbari, C. Cartalis, D. Kolokotsa, A. Muscio, A.L. Pisello, F. Rossi, M. Santamouris, A. Synnefa, N.H. Wong, M. Zinzi, Local climate change and urban heat island mitigation techniques – the state of the art, J. Civ. Eng. Manag. 22 (2016) 1–16.

[5] S. Ramakrishnan, X. Wang, J. Sanjayan, J. Wilson, Thermal performance of buildings integrated with phase change materials to reduce heat stress risks during extreme heatwave events, Appl. Energy. 194 (2017) 410–421.

[6] M.R. Anisur, M.H. Mahfuz, M. a. Kibria, R. Saidur, I.H.S.C. Metselaar, T.M.I. Mahlia, Curbing global warming with phase change materials for energy storage, Renew. Sustain. Energy Rev. 18 (2013) 23–30.

[7] L.F. Cabeza, I. Martorell, L. Miró, A.I. Fernández, C. Barreneche, Introduction to thermal energy storage (TES) systems, in: L.F. Cabeza (Ed.), Adv. Therm. Energy Storage Syst., Elsevier, United Kingdom, 2015: pp. 1–28.

[8] A. Solé, I. Martorell, L.F. Cabeza, State of the art on gas–solid thermochemical energy storage systems and reactors for building applications, Renew. Sustain. Energy Rev. 47 (2015) 386–398.

[9] A. de Gracia, L.F. Cabeza, Phase change materials and thermal energy storage for buildings, Energy Build. 103 (2015) 414–419.

[10] L. Navarro, A. de Gracia, D. Niall, A. Castell, M. Browne, S.J. McCormack, P. Griffiths, L.F. Cabeza, Thermal energy storage in building integrated thermal systems: A review. Part 2. Integration as passive system, Renew. Energy. 85 (2016) 1334–1356.

[11] J. Pereira da Cunha, P. Eames, Thermal energy storage for low and medium temperature applications using phase change materials – A review, Appl. Energy. 177 (2016) 227–238.

[12] H. Mehling, L.F. Cabeza, Heat and cold storage with PCM: an up to date introduction into basics and applications, 1st ed, Springer, New York, 2008.

[13] K. Belz, F. Kuznik, K.F. Werner, T. Schmidt, W.K.L. Ruck, Advances in Thermal Energy Storage Systems, Elsevier, 2015.

[14] M. Alizadeh, S.M. Sadrameli, Development of free cooling based ventilation technology for buildings : Thermal energy storage (TES) unit , performance enhancement

techniques and design considerations – A review, Renew. Sustain. Energy Rev. 58 (2016) 619–645.

[15] F. Kuznik, D. David, K. Johannes, J.J. Roux, A review on phase change materials integrated in building walls, Renew. Sustain. Energy Rev. 15 (2011) 379–391.

[16] B. Zalba, J.M. Marín, L.F. Cabeza, H. Mehling, Review on thermal energy storage with phase change: materials, heat transfer analysis and applications, Appl. Therm. Eng. 23 (2003) 251–283.

[17] L.F. Cabeza, a. Castell, C. Barreneche, a. de Gracia, a. I. Fernández, Materials used as PCM in thermal energy storage in buildings: A review, Renew. Sustain. Energy Rev. 15 (2011) 1675–1695.

[18] C. Barreneche, H. Navarro, S. Serrano, L.F. Cabeza, a. I. Fernández, New Database on Phase Change Materials for Thermal Energy Storage in Buildings to Help PCM Selection, Energy Procedia. 57 (2014) 2408–2415.

[19] A.M. Khudhair, M.M. Farid, A review on energy conservation in building applications with thermal storage by latent heat using phase change materials, Energy Convers. Manag. 45 (2004) 263–275.

[20] S.A. Memon, Phase change materials integrated in building walls: A state of the art review, Renew. Sustain. Energy Rev. 31 (2014) 870–906.

[21] I. Mandilaras, M. Stamatiadou, D. Katsourinis, G. Zannis, M. Founti, Experimental thermal characterization of a Mediterranean residential building with PCM gypsum board walls, Build. Environ. 61 (2013) 93–103.

[22] L. Bianco, V. Serra, S. Fantucci, M. Dutto, M. Massolino, Thermal insulating plaster as a solution for refurbishing historic building envelopes: First experimental results, Energy Build. 95 (2015) 86–91.

[23] L.F. Cabeza, C. Castellón, M. Nogués, M. Medrano, R. Leppers, O. Zubillaga, Use of microencapsulated PCM in concrete walls for energy savings, Energy Build. 39 (2007) 113–119.

[24] C. Barreneche, a. I. Fernández, M. Niubó, J.M. Chimenos, F. Espiell, M. Segarra, C. Solé, L.F. Cabeza, Development and characterization of new shape-stabilized phase change material (PCM) - Polymer including electrical arc furnace dust (EAFD), for acoustic and thermal comfort in buildings, Energy Build. 61 (2013) 210–214.

[25] R. Vicente, T. Silva, Brick masonry walls with PCM macrocapsules: An experimental approach, Appl. Therm. Eng. 67 (2014) 24–34.

[26] S.G. Jeong, J. Jeon, J. Seo, J.H. Lee, S. Kim, Performance evaluation of the microencapsulated PCM for wood-based flooring application, Energy Convers. Manag. 64 (2012) 516–521.

[27] L. Navarro, A. de Gracia, A. Castell, S. Álvarez, L.F. Cabeza, PCM incorporation in a

concrete core slab as a thermal storage and supply system: Proof of concept, Energy Build. 103 (2015) 70–82.
[28] L. Royon, L. Karim, A. Bontemps, Thermal energy storage and release of a new component with PCM for integration in floors for thermal management of buildings, Energy Build. 63 (2013) 29–35.
[29] Project Profile - DELTA® Phase Change Materials, (2017). http://www.cosella-dorken.com/bvf-ca-en/projects/pcm/kempen.php (accessed April 19, 2017).
[30] Phase-Change GlassX Windows Offer Amazing Performance | Inhabitat - Sustainable Design Innovation, Eco Architecture, Green Building, (2017). http://inhabitat.com/phase-change-glassx-windows-offer-amazing-performance/ (accessed April 19, 2017).
[31] L. Navarro, A. de Gracia, S. Colclough, M. Browne, S.J. McCormack, P. Griffiths, L.F. Cabeza, Thermal energy storage in building integrated thermal systems: A review. Part 1. active storage systems, Renew. Energy. 88 (2016) 526–547.
[32] F. Souayfane, F. Fardoun, P.-H. Biwole, Phase change materials (PCM) for cooling applications in buildings: A review, Energy Build. 129 (2016) 396–431.
[33] E. Osterman, V. Butala, U. Stritih, PCM thermal storage system for "free" heating and cooling of buildings, Energy Build. 106 (2015) 125–133.
[34] R. Baetens, B.P. Jelle, A. Gustavsen, Phase change materials for building applications: A state-of-the-art review, Energy Build. 42 (2010) 1361–1368.
[35] H. Akeiber, P. Nejat, M.Z.A. Majid, M.A. Wahid, F. Jomehzadeh, I.Z. Famileh, J.K. Calautit, B.R. Hughes, S.A. Zaki, A review on phase change material (PCM) for sustainable passive cooling in building envelopes, Renew. Sustain. Energy Rev. 60 (2016) 1470–1497.
[36] S.A. Memon, Phase change materials integrated in building walls: A state of the art review, Renew. Sustain. Energy Rev. 31 (2014) 870–906.
[37] H. Jamil, M. Alam, J. Sanjayan, J. Wilson, Investigation of PCM as retrofitting option to enhance occupant thermal comfort in a modern residential building, Energy Build. 133 (2016) 217–229.
[38] L.F. Cabeza, A. de Gracia, Thermal energy storage (TES) systems for cooling in residential buildings, in: L.F. Cabeza (Ed.), Adv. Therm. Energy Storage Syst., Elsevier, 2015: pp. 549–572.
[39] D.B. Crawley, Building Performance Simulation : a Tool for Policymaking, University of Strathclyde,Glasgow, Scotland, UK, 2008. https://www.strath.ac.uk/media/departments/mechanicalengineering/esru/research/phdmphilprojects/crawley_thesis.pdf (accessed April 19, 2017).
[40] D.B. Crawley, Estimating the impacts of climate change and urbanization on building

performance, J. Build. Perform. Simul. 1 (2008) 91–115.

[41] H. Samuelson, S. Claussnitzer, A. Goyal, Y. Chen, A. Romo-Castillo, Parametric energy simulation in early design: High-rise residential buildings in urban contexts, Build. Environ. 101 (2016) 19–31.

[42] Z. Li, S.J. Quan, P.P.-J. Yang, Energy performance simulation for planning a low carbon neighborhood urban district: A case study in the city of Macau, Habitat Int. 53 (2016) 206–214.

[43] G. Evola, L. Marletta, F. Sicurella, A methodology for investigating the effectiveness of PCM wallboards for summer thermal comfort in buildings, Build. Environ. 59 (2013) 517–527.

[44] J. Lei, J. Yang, E.-H. Yang, Energy performance of building envelopes integrated with phase change materials for cooling load reduction in tropical Singapore, Appl. Energy. 162 (2016) 207–217.

[45] M. Alam, H. Jamil, J. Sanjayan, J. Wilson, Energy saving potential of phase change materials in major Australian cities, Energy Build. 78 (2014) 192–201.

[46] M. Saffari, A. de Gracia, S. Ushak, L.F. Cabeza, Economic impact of integrating PCM as passive system in buildings using Fanger comfort model, Energy Build. 112 (2016) 159–172.

[47] A.-T. Nguyen, S. Reiter, P. Rigo, A review on simulation-based optimization methods applied to building performance analysis, Appl. Energy. 113 (2014) 1043–1058.

[48] N. Soares, a. R. Gaspar, P. Santos, J.J. Costa, Multi-dimensional optimization of the incorporation of PCM-drywalls in lightweight steel-framed residential buildings in different climates, Energy Build. 70 (2014) 411–421.

[49] T. Nguyen Van, A. Miyamoto, D. Trigaux, F. De Troyer, Cost and comfort optimisation for buildings and urban layouts by combining dynamic energy simulations and generic optimisation tools, in: WIT Trans. Built Environ., WITPress, 2014: pp. 81–92.

[50] R. Evins, A review of computational optimisation methods applied to sustainable building design, Renew. Sustain. Energy Rev. 22 (2013) 230–245.

[51] F. Roberti, U.F. Oberegger, E. Lucchi, A. Troi, Energy retrofit and conservation of a historic building using multi-objective optimization and an analytic hierarchy process, Energy Build. 138 (2017) 1–10.

[52] R. Wu, G. Mavromatidis, K. Orehounig, J. Carmeliet, Multiobjective optimisation of energy systems and building envelope retrofit in a residential community, Appl. Energy. 190 (2017) 634–649.

[53] ASHRAE 90.1 Prototype Building Models Mid-rise Apartment, (2017). https://www.energycodes.gov/901-prototype-building-models-mid-rise-apartment (accessed April 19, 2017).

[54] B.A. Thornton, M.I. Rosenberg, E.E. Richman, W. Wang, Y. Xie, J. Zhang, H. Cho, V. V. Mendon, R.A. Athalye, B. Liu, Achieving the 30% Goal: Energy and Cost Savings Analysis of Ashrae Standard 90.1-2010, 2011.
[55] S. Goel, M. Rosenberg, R. Athalye, Y. Xie, W. Wang, R. Hart, J. Zhang, V. Mendon, Enhancements to ASHRAE Standard 90 . 1 Prototype Building Models, (2014).
[56] J. Kośny, PCM-Enhanced Building Components - An application of Phase Change Materials in Building Envelopes and Internal Structures, Springer International Publishing, Switzerland, 2015.
[57] P.W. Egolf, H. Manz, Theory and modeling of phase change materials with and without mushy regions, Int. J. Heat Mass Transf. 37 (1994) 2917–2924.
[58] Helmut E.Feustel, Simplified Numerical Description of Latent Storage Characteristics for Phase Change Wallboard, Indoor Environment Program,Energy and Environment Division,Lawrence Berkeley Laboratory,University of California, California, 1995.
[59] R. and A.-C.E. American Society of Heating, Standard 90.1-2013. Energy Standard for Buildings Except Low-Rise Residential Buildings, Am. Soc. Heating, Refrig. Air-Conditioning Eng. Inc. 2013 (2013) 278.
[60] BS EN 15251:2007, Indoor environmental input parameters for design and assessment of energy performance of buildings- addressing indoor air quality , thermal environment , lighting and acoustics Contents, (2007) 1–52.
[61] D.B. Crawley, L.K. Lawrie, F.C. Winkelmann, W.F. Buhl, Y.J. Huang, C.O. Pedersen, R.K. Strand, R.J. Liesen, D.E. Fisher, M.J. Witte, J. Glazer, EnergyPlus: Creating a new-generation building energy simulation program, Energy Build. 33 (2001) 319–331.
[62] D.B. Crawley, C.O. Pedersen, L.K. Lawrie, F.C. Winkelmann, Energy plus: Energy simulation program, ASHRAE J. 42 (2000) 49–56.
[63] EnergyPlus Engineering Reference, EnergyPlus Engineering Reference: The Reference to EnergyPlus Calculations, US Dep. Energy. (2016) 1444.
[64] Guide for Module Developers Everything You Need to Know about Developing Modules and Modifying EnergyPlus, October. (2010).
[65] D.B. Crawley, J.W. Hand, M. Kummert, B.T. Griffith, Contrasting the capabilities of building energy performance simulation programs, Build. Environ. 43 (2008) 661–673.
[66] US Department of Energy, EnergyPlus. (2017). https://energyplus.net/ (accessed April 19, 2017).
[67] EnergyPlus v8.7 Input Output Reference: The Encyclopedic Reference to EnergyPlus Input and Output, (2017).
[68] P.C. Tabares-velasco, C. Christensen, M. Bianchi, C. Booten, Verification and Validation of EnergyPlus Conduction Finite Difference and Phase Change Material Models for Opaque Wall Assemblies, (2012).

[69] D.B. Crawley, C.O. Pedersen, F.C. Winkelmann, M.J. Witte, R.K. Strand, R.J. Liesen, W.F. Buhl, Energyplus: New , Capable and Linked, J. Archit. Plann. Res. 21 (2004) 292–302.

[70] P.C. Tabares-Velasco, C. Christensen, M. Bianchi, Verification and validation of EnergyPlus phase change material model for opaque wall assemblies, Build. Environ. 54 (2012) 186–196.

[71] M. Tabares-Velasco, P.C Christensen, C Bianchi, Validation Methodology to Allow Simulated Peak Reduction and Energy Performance Analysis of Residential Building Envelope with Phase Change Materials, in: 2012 ASHRAE Annu. Conf. June 23-27, National Renewable Energy Laboratory, San Antonio, Texas, 2012.

[72] D. Pan, M. Chan, S. Deng, Z. Lin, The effects of external wall insulation thickness on annual cooling and heating energy uses under different climates, Appl. Energy. 97 (2012) 313–318.

[73] F. Kuznik, J. Virgone, Experimental assessment of a phase change material for wall building use, Appl. Energy. 86 (2009) 2038–2046.

[74] M. Auzeby, S. Wei, C. Underwood, J. Tindall, C. Chen, H. Ling, R. Buswell, Effectiveness of Using Phase Change Materials on Reducing Summer Overheating Issues in UK Residential Buildings with Identification of Influential Factors, Energies. 9 (2016) 605.

[75] J.S. Sage-Lauck, D.J. Sailor, Evaluation of phase change materials for improving thermal comfort in a super-insulated residential building, Energy Build. 79 (2014) 32–40.

[76] M. Wetter, Design Optimization with GenOpt, Build. Energy Simul. User News. 21 (2000) 200. http://simulationresearch.lbl.gov/wetter/download/userNews-2000.pdf (accessed April 19, 2017).

[77] M. Wetter, GenOpt - A Generic Optimization Program, Seventh Int. IBPSA Conf. (2001) 601–608.

[78] R. Hooke, T.A. Jeeves, Direct Search'' Solution of Numerical and Statistical Problems, J. ACM. 8 (1961) 212–229.

[79] M. Wetter, GenOpt(R) Generic Optimization Program User Manual Version 3.1.1, (2016).

[80] M. Wetter, J. Wright, A comparison of deterministic and probabilistic optimization algorithms for nonsmooth simulation-based optimization, Build. Environ. 39 (2004) 989–999.

[81] R.M. Lewis, V. Torczon, M.W. Trosset, Direct search methods: then and now, J. Comput. Appl. Math. 124 (2000) 191–207.

[82] M. Kottek, J. Grieser, C. Beck, B. Rudolf, F. Rubel, World map of the Köppen-Geiger

climate classification updated, Meteorol. Zeitschrift. 15 (2006) 259–263.
[83] M. Blumthaler, Solar Radiation of the High Alps, in: Plants Alp. Reg., Springer Vienna, Vienna, 2012: pp. 11–20.
[84] J. Kośny, A. Fallahi, N. Shukla, E. Kossecka, R. Ahbari, Thermal load mitigation and passive cooling in residential attics containing PCM-enhanced insulations, Sol. Energy. 108 (2014) 164–177.
[85] P. Marin, M. Saffari, A. de Gracia, X. Zhu, M.M. Farid, L.F. Cabeza, S. Ushak, Energy savings due to the use of PCM for relocatable lightweight buildings passive heating and cooling in different weather conditions, Energy Build. 129 (2016) 274–283.
[86] X. Mi, R. Liu, H. Cui, S.A. Memon, F. Xing, Y. Lo, Energy and economic analysis of building integrated with PCM in different cities of China, Appl. Energy. 175 (2016) 324–336.
[87] F. Kuznik, J.P. Arzamendia Lopez, D. Baillis, K. Johannes, Phase change material wall optimization for heating using metamodeling, Energy Build. 106 (2015) 216–224.